Journal of Materials and Environmental Sciences
ISSN : 2028-2508

JMES, 2017 Volume 8, Issue 7, Page 2455-2467

http://www.jmaterenvironsci.com /

Experimental and theoretical studies of Alizarin as corrosion inhibitor for mild steel in 1.0 M HCl solution

L. Saqalli[1], M. Galai[2], F. Benhiba[3], N. Gharda[1], N. Habbadi[1], R.Ghailane[1], M. Ebn Touhami[2], Y. Peres-lucchese[4], A. Souizi[1], R. Touir[2,5*]

[1] *Laboratory of Organic Synthesis, Organometallic and Theory, Faculty of Science, Ibn Tofail University, PO Box 133, 14 000 Kenitra, Morocco.*

[2] *Laboratory of Materials Engineering and Environment: Modeling and Application, Faculty of Science, Ibn Tofail University, PO Box 133, 14000, Kenitra, Morocco.*

[3] *Laboratory of separation methods, Faculty of Science, Ibn Tofail University, PO Box 133, 14000, Kenitra, Morocco.*

[4] *Chemical Engineering Laboratory UMR / UPS, Toulouse University, PO Box 84234, 4 Emile Monso went, F-31432 Toulouse Cedex 4, France.*

5 Regional center of education and training (CRMEF), Avenue Allal al-Fassi, Madinat Al Irfane PO Box 6210, Rabat, Morocco.

Received 15 Jun 2016,
Revised 01 Nov 2016,
Accepted 03 Nov 2016

Keywords

- ✓ Corrosion inhibitor;
- ✓ Mild steel;
- ✓ Alizarin;
- ✓ Weight loss;
- ✓ Electrochemical measurements;
- ✓ DFT.

touir8@yahoo.fr & *touir8@gmail.com*
Tel: +212 670 526 959.

Abstract

The corrosion inhibition of mild steel in 1.0 M HCl solution by Alizarin was investigated using weight loss and electrochemical measurements. The results indicate that the studied compound exhibits good performance as inhibitor for mild steel corrosion in 1.0 M HCl solution and its inhibition efficiency increased with concentration to reach a maximum of 91 % at 10^{-3} M (optimum concentration). The potentiodynamic polarization curves showed that Alizarin acts as a cathodic type inhibitor. It is found also that the inhibition efficiency of this compound decreased with temperature to reach a minimum of 54.3 % at 10^{-3} M at 328 K. In the other, it is shown that the inhibition efficiency increased with immersion time until 4 h to get 0.89 % and decreased after this time to attain 66.1% at 12 h at the optimum concentration. So, the adsorption of Alizarin obeys to the Langmuir adsorption isotherm. In addition, the apparent activation energy, enthalpy, entropy and the free energy were determined and discussed. Finally, the quantum chemical parameters were determined using density functional theory (DFT) method to correlate the calculated structural and electronic parameters of Alizarin with its corrosion inhibition efficiency. The obtained results indicated a good agreement between experimental and theoretical studies.

1. Introduction

The hydrochloric acid solution is one of the most-used acid for degreasing, descaling, pickling,…etc [**1**,**2**]. So, this acid causes the metallic degradation, due to its aggressiveness either by chemical or electrochemical reactions. To prevent it, many inhibitors were used which prove to be not expensive and an easy method to implement [**3**, **4**]. Thus, organic compounds containing hetero atoms and aromatic cycles have been reported to be effective inhibitors for the corrosion of the materials in aggressive environments [**5-10**]. The object of several studies was to use organic compounds as inhibitors of mild steel corrosion in HCl solutions such as Methyl green [**11**], Thymol blue [**12**], Alizarin yellow GG [**13**], Alizarin violet 3B [**14**], the Red Alizarin ARS [**15**] and indigo dye [**16**]. However, the inhibition efficiency depends on the chemical nature of the inhibitor and the adsorption mode which occurs by the formation of a protective layer at the metallic surface [**17**].

In the other hand, quantum chemical calculations have been widely used to study reaction mechanisms and to interpret the experimental results as well as to resolve chemical ambiguities [**10**, **18, 19**].

The aim of this work is to study the effect of Alizarin on the corrosion inhibition of mild steel in HCl solution using weight loss and electrochemical measurements. We have also studied its performance in the temperature range from 298 K to 328 K and we have determined the kinetic and thermodynamic parameters and interpreted. On the other hand, the quantum chemical calculations were performed to determine the global reactivity indices of the used inhibitor.

2. Experimental details:

2.1. Experimental study:

The chemical composition of mild steels sample is shown in Table 1. The specimen's surface was prepared by polishing with emery paper at different grit sizes (from 180 to 1200), rinsing with distilled water, degreasing in ethanol, and drying at hot air. The used steels specimens have a rectangular form 1.4 cm × 1 cm × 0.3 cm. The immersion time for weight loss was 2 h, 4 h, 8 h, 16 h or 24 h. After immersion period, the specimens were cleaned according to ASTM G-81 and reweighed to 10^{-4} g for determining corrosion rate [**20**]. The aggressive solution of 1.0 M HCl was prepared by dilution of analytical grade 37 % HCl with distilled water. The molecular formula of the examined inhibitor is shown in Table 2. The inhibition efficiency, η_w (%), is determined as follows :

$$\eta_\omega\% = \frac{\omega^0_{corr} - \omega_{corr}}{\omega^0_{corr}} \times 100 \quad (1)$$

where ω^0_{corr} and ω_{corr} are the corrosion rates in the absence and presence of inhibitors, respectively.

For electrochemical measurements, the electrolysis cell was a borrosilcate glass (Pyrex®) cylinder closed by a cap with five apertures. Three of them were used for the electrode insertions. The working electrode was pressure-fitted into a polytetrafluoroethylene holder (PTFE) exposing only 1 cm^2 of area to the solution. Platinum and saturated calomel were used as counter and reference electrode (SCE), respectively. All potentials were measured against the last electrode. The potentiodynamic polarization curves were recorded by changing the electrode potential automatically from negative values to positive values versus E_{corr} using a Potentiostat/Galvanostat type PGZ 100, at a scan rate of 1 mV/s after 1 h of immersion time until reaching steady state. The test solution was thermostatically controlled at 298±1 K in air atmosphere without bubbling. To evaluate corrosion kinetic parameters, a fitting by Stern-Geary equation was used [**21**]. The corrosion inhibition efficiency is evaluated from the corrosion current densities values using the relationship (2):

$$\eta_{PP} = \frac{i^0_{corr} - i_{corr}}{i^0_{corr}} \times 100 \quad (2)$$

where i^0_{corr} and i_{corr} are the corrosion current densities values without and with inhibitor, respectively.

The electrochemical impedance spectroscopy measurements were carried out using a transfer function analyzer, with a small amplitude a.c. signal (10 mV rms), over a frequency domain from 100 kHz to 100 mHz with five points per decade. The results were then analyzed in terms of an equivalent electrical circuit using EC-Lab software. The inhibiting efficiency derived from EIS, η_{EIS}, calculated using the following equation (3):

$$\eta_{EIS} = \frac{R_{ct} - R^0_{ct}}{R_{ct}} \times 100 \quad (3)$$

where R^0_{ct} and R_{ct} are the charge transfer resistance values in the absence and presence of inhibitor, respectively.

In order to ensure reproducibility, all experiments were repeated three times. The evaluated inaccuracy did not exceed 10 %.

Table 1 : Chemical composition of carbon steel in wt %.

C	Si	Mn	Cr	Mo	Ni	Al	Cu	Co	V	W	Fe
0.11	0.24	0.47	0.12	0.02	0.1	0.03	0.14	<0.0012	<0.003	0.06	Balance

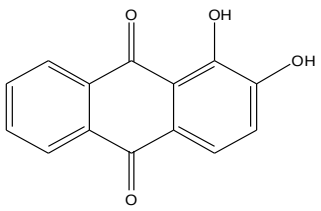

Figure 1: Chemical structure of Alizarin.

2.2. Computational method

The complete optimization of the geometrical structure of the Alizarin was performed using the Density Functional Theory (DFT) with the Beck's three parameter exchange functional and the Lee–Yang–Parr non-

local correlation functional (B3LYP) [**22**, **23**] combined to standard basis set of atomic orbital 6-31G(d) as implemented in Gaussian 03 program package [**24**]. This choice is based in the fact that the DFT method is proved as a very useful technique to probe the inhibitor/surface interaction as well as to analyze the experimental data [**25**]. In order to examine the solvent effect on the geometrical structure and in the electronic properties one opt to take into account of this effect by using the polarized continuum model (PCM) [**26**] and water as solvent. In this model, the solvent was treated as a continuum dielectric media and the solute is considered as a trapped molecule in a cavity surrounded by solvent.

The complete geometry optimization of the Alizarin was determined in gas and aqueous phases. The stability of the optimized geometry of the molecular structure was confirmed by harmonic vibrational wave numbers calculated using analytic second derivatives which have shown the absence of imaginary frequency modes.

The HOMO energy is related to the ionization potential (I) whereas the LUMO energy is linked to the electron affinity (A), as follows:

$$I = -E_{HOMO} \quad (4)$$

$$I = -E_{LUMO} \quad (5)$$

The energetic gap is determined as follow:

$$\Delta E = E_{LUMO} - E_{HOMO} \quad (6)$$

Then, the electronegativity (χ), the chemical potential (μ) and the global hardness (η) were evaluated, based on the finite difference approximation, as linear combinations of the calculated I and A:

$$\chi = -\mu = \frac{I + A}{2} \quad (7)$$

$$\eta = \frac{I - A}{2} \quad (8)$$

The fraction of transferred electrons (ΔN), evaluating the electronic flow in a reaction of two systems with different electronegativities in particular case a metallic surface and an inhibitor molecules, was calculated according to Pearson theory [**27**] as follows:

$$\Delta N = \frac{\chi_{Fe} - \chi_{inh}}{2(\eta_{Fe} + \eta_{inh})} \quad (9)$$

where the indices Fe and inh refer to iron atom and inhibitor molecule, respectively.

3. Results and discussion:

3.1. Potentioidynamic polarization curves

The potentiodynamic polarization curves of mild steel in 1.0 M HCl in the absence and presence of different concentrations of Alizarin are shown in Figure 2 . Their electrochemical parameters are given in Table 2. These results show that Alizarin brings down (i_{corr}) value at all concentrations and the minimum values was obtained at 10^{-3} M. Moreover, it is noted that this compound causes a significant shift in (E_{corr}) values to cathodic values with a decrease in the current densities values indicating that it is a cathodic type inhibitor in 1.0 M HCl. It is noted that the cathodic and anodic Tafel slopes (β_a and β_c) change with inhibitor indicating a change in the iron dissolution and hydrogen evolution reactions.

3.2. Electrochemical impedance spectroscopy (EIS)

Figure 3 shows the Nyquist plots obtained for mild steel in 1.0 M HCl in the absence and presence of different concentrations of Alizarin at the open circuit potential. Their corresponding parameters are shown in Table 3. In addition the obtained results can be interpreted using the equivalent circuit presented in Figure 4, which has been used previously to model the iron/acid solution interface **[28]**. It is apparent from these plots that the obtained impedance was composed of one capacitive loop which its diameter was significantly changed after inhibitors addition and the greatest effect was observed at 10^{-3} M of Alizarin. In addition, these impedance diagrams are not perfect semicircles and this difference has been attributed to frequency dispersion **[29]**.

However, the inhibitors addition is found to enhance R_{ct} values and bring down C_{dl} values. These observations clearly bring out the fact that the mild steel corrosion in 1.0 M HCl is controlled by a charge transfer process and the corrosion inhibition occurs through the adsorption of the Alizarin on mild steel surface. Decrease in the C_{dl} values, with can result from a decrease in local dielectric constant and/or an increase in courant density, the thickness of the electrical double layer, suggested that the Alizarin molecules function by adsorption at the metal/solution interface **[30**, **31]**.

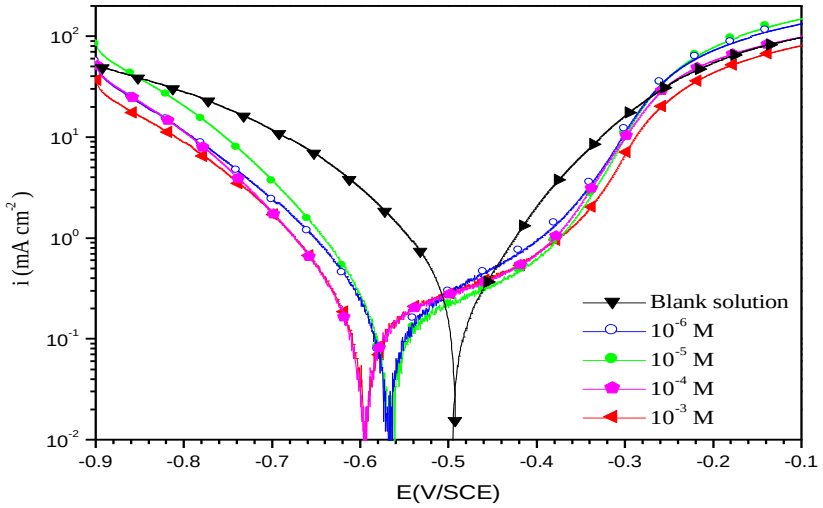

Figure 2: Potentiodynamic polarization curves for mild steel in 1.0 M HCl without and with different concentrations of Alizarin at 298K.

Table 2: Electrochemical parameters of mil steel at various concentrations of Alizarin in 1.0 M HCl and **their** corresponding inhibition efficiency.

Inhibitor	Conc. (M)	E_{corr} (mV/SCE)	βa (mV dec^{-1})	–βc (mV dec^{-1})	i_{corr} (µA cm^{-2})	η_{PP} (%)
Blank	00	-498.0	94	102.0	455.50	-----
Alizarin	10^{-6}	-570.9	120	78.4	100.50	79.1
	10^{-5}	-568.3	123	56.2	67.31	84.8
	10^{-4}	-597.7	126	53.3	62.30	86.1
	10^{-3}	-596.9	124	46.3	52.54	88.5

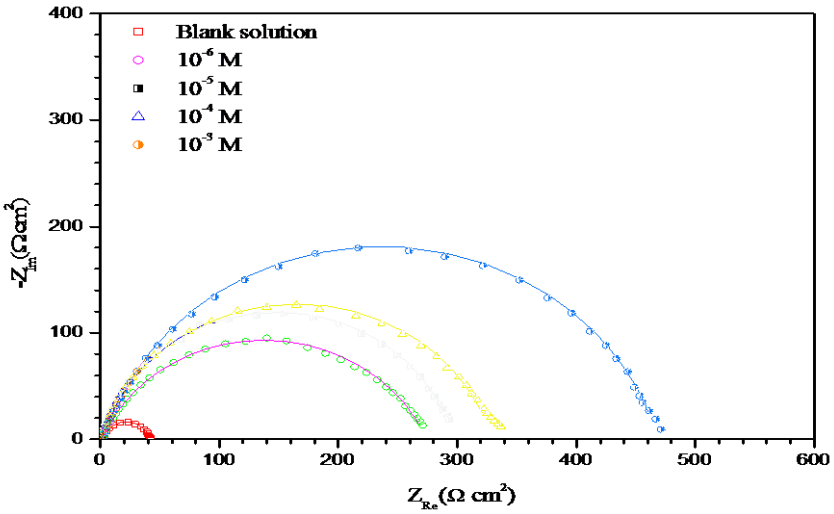

Figure 3: Nyquist plots of mild steel corrosion in 1.0 M HCl without and with different concentrations of Alizarin at open circuit potential. Symbols: Experimental data; Lines: Fitting data.

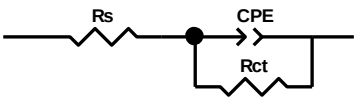

Figure 4: Electrochemical equivalent circuit used to fit the impedance measurements.

In addition, the increase in n_{dl} with inhibitor concentration can be attributed to the increase of surface homogeneity linked to the adsorption of Alizarin molecules on the metallic surface **[32**, **33]**. The similar behaviors were obtained in our pervious study for the low carbon steel in simulated cooling water **[34]**. Likewise, the value of the relaxation time constant, ($\tau_{ct} = R_{ct} \times C_{dl}$), increases globally with Alizarin

concentration, i.e., the time of adsorption process becomes therefore much higher which means a slow adsorption process **[35]**. It is noted a good agreement with results obtained from potentiodynamic polarization measurements.

Table 3: Electrochemical parameters and inhibitory efficiency for mild steel in 1.0 M HCl at different concentrations of Alizarin.

	Conc. (M)	R_{ct} (Ω cm^2)	C_{dl} (μF cm^{-2})	n_{dl}	τ_{ct} (ms)	η_{EIS} (%)
Blank	00	38.87±0.82	255.3±0.53	0.76±0.01	9.92	-
Alizarin	10^{-6}	272.8±0.47	143.10±0.49	0.84±0.01	39.04	85.7
	10^{-5}	294.5±0.57	97.44±0.29	0.84±0.01	28.70	86.8
	10^{-4}	327.7±0.51	95.78±0.16	0.87±0.01	31.39	88.1
	10^{-3}	464.4±0.63	93.57±0.52	0.89±0.01	43.45	91.6

3.3. Activation parameters

The effect temperature on the corrosion inhibition of mild steel in free acid and inhibited 1.0 M HCl was studied in the temperature range 298-328 K using weight loss measurements. The obtained results are presented in Table 4. It is noted that the corrosion rate of mild steel in free solution increase with temperature. It is noted also that the inhibition efficiency was decreased slightly by the increasing temperature. This finding can be explained by the fact that the enhanced effect of temperature on the dissolution process of mild steel in acidic media, increases the corrosion rate, and/or the partial desorption of the inhibitor from the metal surface, causing consequentially a decrease of the inhibitory efficiency [**36**, **37**]

In addition, the dependence of logarithm of corrosion rates (Ln ω_{corr}) on the reciprocal of absolute temperature (1/T) for 1.0 M HCl for blank solution and in the presence of different concentration of Alizarin was examined. Linear plots were obtained (Figure 5), which indicate it follows Arrhenius equation:

$$Ln\omega_{corr} = -\frac{E_a}{RT} + LnA \qquad (10)$$

where A is the Arrhenius pre-exponential constant, R is the universal gas constant, E_a is the apparent activation energy and T is the absolute temperature. The values obtained from the slope of the linear plots are shown in Table 5. All the linear regression coefficients are close to 1, indicating that the mild steel corrosion in hydrochloric acid can be elucidated using the kinetic model. As observed from the Table 5, the E_a increased in the presence of Alizarin compared to the uninhibited solution (Blank solution). The increase in E_a in the presence of Alizarin may be interpreted as physical adsorption. Indeed, a higher energy barrier for the corrosion process in the inhibited solution is associated with physical adsorption or weak chemical bonding between the inhibitors species and the mild steel surface [**37**, **38**]. Szauer et al. explained that the increase in activation energy can be attributed to an appreciable decrease in the adsorption of the inhibitor on the mild steel surface with the increase in temperature [**39**].

The other kinetic parameters such as enthalpy of adsorption (ΔH_a) and entropy of adsorption (ΔS_a) were obtained from transition state equation:

$$\mathrm{Ln}\,\frac{\omega_{corr}}{T} = \ln\left(\frac{R}{Nh}\right) + \left(\frac{\Delta S_a}{R}\right) - \frac{\Delta H_a}{RT} \qquad (11)$$

where ω_{corr} is the corrosion rate, h the Plank's constant and N is Avogrado's number, ΔH_a the enthalpy of activation and ΔS_a the entropy of activation.

Figure 6 shows the variation of Ln (ω_{corr}/T) function (1/T) as a straight line with a slope of ($-\Delta H_a$/ R) and the intersection with the y-axis is [Ln(R/Nh) + (ΔS_a / R)]. From these relationships, values of ΔS_a and ΔH_a can be calculated. The activation parameters (ΔH_a and ΔS_a) calculated from the slopes of Arrhenius lines in the absence and presence of our inhibitors are summarized in Table 5.

Inspection of these data reveals that the ΔH_a value for dissolution reaction of mild steel in 1.0 M HCl in the presence of Alizarin is higher in the absence of inhibitors. The positive signs of ΔH_a values reflect the endothermic nature of the mild steel dissolution process suggesting that the dissolution of mild steel is difficult [**40**] in the presence of Alizarin. All values of E_a are larger than the analogous values of ΔH_a indicating that the corrosion process must involved a gaseous reaction, simply the hydrogen evolution reaction, associated with a decrease in the total reaction volume [**41**]. Additionally, Table 5 shows that the values of ΔS_a increase in presence of inhibitor compared to blank solution, which mean an increase in disorder takes place during the course of the transition from reactant to the activated complex during the corrosion process [**42**, **43**].

Table 4: Gravimetric data for mild steel in 1.0 M HCl in the presence of Alizarin at different concentrations and at different temperatures.

T (K)	Conc . (M)	ω_{corr} (mg h^{-1} cm^{-2})	η_{ω} (%)	θ
298	00	0.1977	-	-
	10^{-6}	0.0609	69.2	0.6920
	10^{-5}	0.0478	75.8	0.7582
	10^{-4}	0.0439	77.8	0.7779
	10^{-3}	0.0219	88.9	0.8892
308	00	0.3954	-	-
	10^{-6}	0.2753	30.4	0.3037
	10^{-5}	0.2290	42.1	0.4208
	10^{-4}	0.1900	51.9	0.5195
	10^{-3}	0.1318	67.0	0.6666
318	00	1.4339	-	-
	10^{-6}	1.0018	30.1	0.3013
	10^{-5}	0.8680	39.5	0.3947
	10^{-4}	0.7798	45.6	0.4562
	10^{-3}	0.5286	63.1	0.6314
328	00	2.3430	-	-
	10^{-6}	1.8269	22.0	0.2203
	10^{-5}	1.6500	29.6	0.2958
	10^{-4}	1.4187	39.5	0.3945
	10^{-3}	1.0699	54.3	0.5434

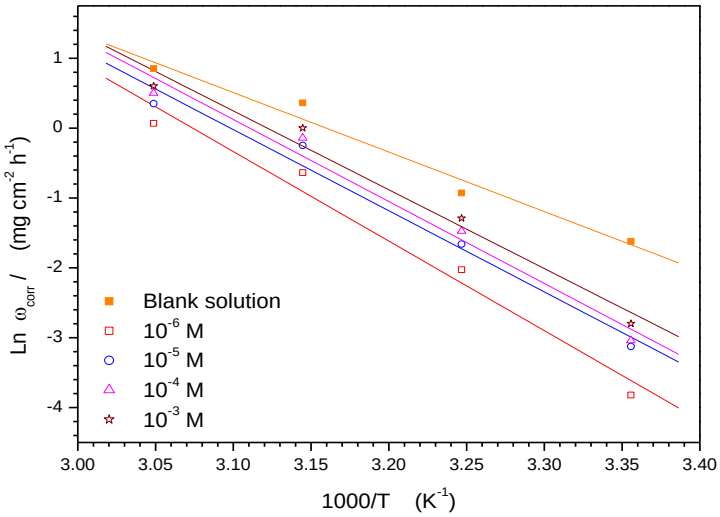

Figure 5: Arrhenius plots for mild steel in 1.0 M HCl without and with different concentration of Alizarin.

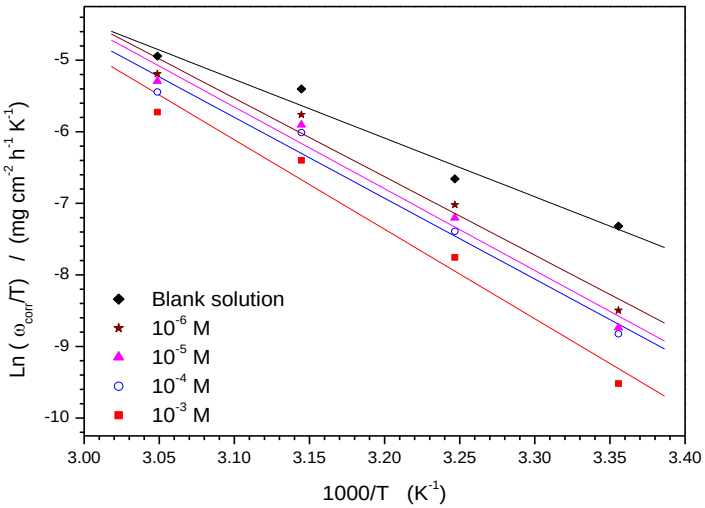

Figure 6: Transition Arrhenius plots for mild steel in 1.0 M HCl solution without and with different concentration of Alizarin.

Table 5 : The values of activation parameters E_a, ΔH_a and ΔS_a for mild steel in 1.0 M HCl without and with different concentration of Alizarin.

Compounds	Conc. (M)	E_a (KJ mol^{-1})	ΔH_a (KJ mol^{-1})	ΔS_a (J K^{-1} mol^{-1})
Blank solution	00	70.85	68.25	-30.41
	10^{-6}	93.89	91.29	38.84
Alizarin	10^{-5}	97.66	95.06	49.48
	10^{-4}	96.66	94.06	45.20
	10^{-3}	106.67	104.07	73.61

3.4. Effect of immersion time :

The corrosion rate values (ω_{corr}) of mild steel in 1.0 M HCl at different concentrations of Alizarin and immersion time at 298 K are presented in Table 6. It is noted that the corrosion rate increased with concentration at all immersion time. This behavior can be attributed to the increase of the covered surface by the molecules with increasing of its concentration. This result is in good agreement with previous works for other inhibitors [**44**]. It is noted also that the inhibition efficiency increased with immersion time until 4 h and became to decrease which can be explained by the physical mode of the inhibitor. This finding was confirmed by the obtained values of ΔG_{ads} such as mentioned in Table 7.

Table 6: Effect of concentration of Alizarin and immersion time on the corrosion inhibition of mild steel 1.0 M HCl at 298 K.

Times (h)	Conc. (M)	ω_{corr} (mg h^{-1} cm^{-2})	η_ω (%)	θ
2	00	0.1900	-	-
	10^{-6}	0.1100	42.1	0.4211
	10^{-5}	0.0890	53.2	0.5316
	10^{-4}	0.0572	69.9	0.6989
	10^{-3}	0.0352	81.5	0.8147
4	00	0.1977	-	-
	10^{-6}	0.0609	69.2	0.6920
	10^{-5}	0.0478	75.8	0.7582
	10^{-4}	0.0439	77.8	0.7779
	10^{-3}	0.0219	88.9	0.8892
8	00	0.2397	-	-
	10^{-6}	0.0995	58.5	0.5849
	10^{-5}	0.0887	62.9	0.6299
	10^{-4}	0.0671	72.0	0.7201
	10^{-3}	0.0347	85.5	0.8552
16	00	0.3720	-	-
	10^{-6}	0.1949	47.6	0.4761
	10^{-5}	0.1678	54.9	0.5489
	10^{-4}	0.1280	65.6	0.6559
	10^{-3}	0.0750	79.8	0.7984
24	00	0.5020	-	-
	10^{-6}	0.3499	30.3	0.3030
	10^{-5}	0.2698	46.3	0.4625
	10^{-4}	0.2159	56.9	0.5699
	10^{-3}	0.1699	66.1	0.6615

3.4. Adsorption isotherm and thermodynamic analysis

The corrosion inhibition of metals us organic compounds was explained by their adsorption which possibly involves two types of interaction with metallic surface (physisorption, chemisorption). So, the adsorption process depends upon the charge and the nature of the metal surface, the chemical structure of inhibitor and the electrolyte type [**45**]. Thus, the physisorption involves weak undirected interactions due to electrostatic attraction between inhibitor and the charge of metallic surface [**46**]. While, the chemisorption process involves charge sharing or charge-transfer from the inhibitor molecules to vacant d-orbitals of the metal surface in order to form a coordinate type bond [**46**].

However, several adsorption isotherms are usually used to describe the adsorption process, include Temkin, Frumkin, Parsons and Flory-Huggins [**47-50**]. The best fit is obtained with the Langmuir isotherm. The Langmuir adsorption isotherm is given by [**51**]

$$\frac{C_{inh}}{\theta} = \frac{1}{K_{ads}} + C_{inh} \qquad (12)$$

where C_{inh} is the equilibrium inhibitor concentration, K_{ads} adsorptive equilibrium constant.

The plots of C_{inh}/θ against C_{inh} at different temperature and immersion time are presented in Figures 7 and 8. They give the straight lines indicating the adsorption of Alizarin on mild steel surface obeys to the Langmuir adsorption isotherm.

Thermodynamic parameters including the heat of adsorption, free energy of adsorption, and entropy of adsorption are important in the explanation of the corrosion inhibition mechanism. The free energy of adsorption (ΔG_{ads}) can be obtained from the equation [**52**]

$$\Delta G_{ads} = -RTLn(55.5K_{ads}) \qquad (13)$$

where R is gas constant and T is absolute temperature of experiment and the constant value of 55.5 is the concentration of water in solution in mol L^{-1}.

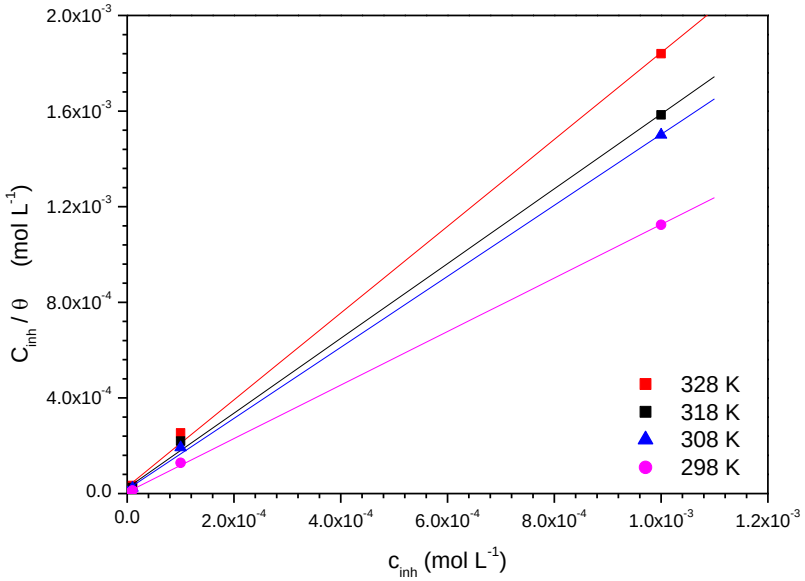

Figure 7: Langmuir isotherm adsorption mode of Alizarin on the mild steel surface in 1.0 M HCl at different temperature.

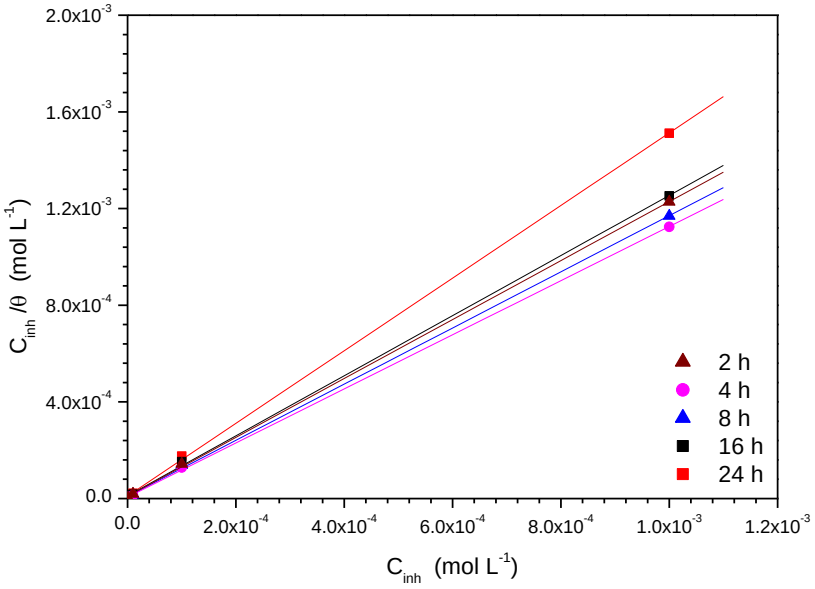

Figure 8: Langmuir isotherm adsorption mode of Alizarin on the mild steel surface in 1.0 M HCl at different immersion time.

The enthalpy and entropy of adsorption (ΔH_{ads} and ΔS_{ads}) can be calculated using the following equations [**53**]:

$$\text{Ln } K_{ads} = -\frac{\Delta H_a}{RT} + cons\tan t \quad (14)$$

$$\Delta G_{ads} = \Delta H_{ads} - T\Delta S_{ads} \quad (15)$$

Figure 9 represents the plots of Ln K_{ads} versus 1/T for Alizarin and the thermodynamic parameters obtained are given in Table 8. The values of ΔG_{ads} are negative ensure the spontaneity of the adsorption process and the stability of the adsorbed layer on the mild steel surface. Generally speaking, the adsorption type is regarded as physisorption if the absolute value of ΔG_{ads} was of the order of 20 kJ mol^{-1} or lower. The inhibition behaviour is attributed to the electrostatic interaction between the organic molecules and iron atom. When the absolute value of ΔG_{ads} is of the order of 40 kJ mol^{-1} or higher, the adsorption could be seen as chemisorption. In this process, the covalent bond is formed by the charge sharing or transferring from the inhibitor molecules to the metal surface [**54**, **55**]. Based on the literature [**56**], the calculated ΔG_{ads} values in this work (Table 7) indicate that the adsorption mechanism of these compounds on mild steel in 1.0 M HCl solution is typical of physisorption in all case an exception in the case of T = 298 K and at 4 h, the obtained value of ΔG_{ads} is near 40 kJ mol^{-1} indicating that the adsorption mechanism Alizarin molecules on mild steel is typical of chemisorption. In the other hand, it has concluded also that the mode of adsorption of this compound depended on the solution temperature.

Table 7: Thermodynamic parameters for the adsorption of Alizarin on mild steel in 1.0 M HCl at different temperature and immersion time.

	T (K)	R^2	Slope	K_{ads}(L mol^{-1})	ΔG_{ads} (kJ mol^{-1})
Alizarin	298	0.9999	1.11	1.68×10^5	-39.79
	308	0.9996	1.48	5.756×10^4	-38.38
	318	0.9993	1.56	4.257×10^4	-38.83
	328	0.9994	1.81	3.483×10^4	-39.50
	Time (h)	R^2	Slope	K_{ads}(L mol^{-1})	ΔG_{ads} (kJ mol^{-1})
	2	0.9999	1.21	1.08×10^5	-38.69
	4	0.9999	1.11	1.68×10^5	-39.79
	8	0.9998	1.16	1.15×10^5	-38.85
	16	0.9998	1.24	9.05×10^4	-38.26
	24	0.9999	1.50	9.3×10^4	-38.33

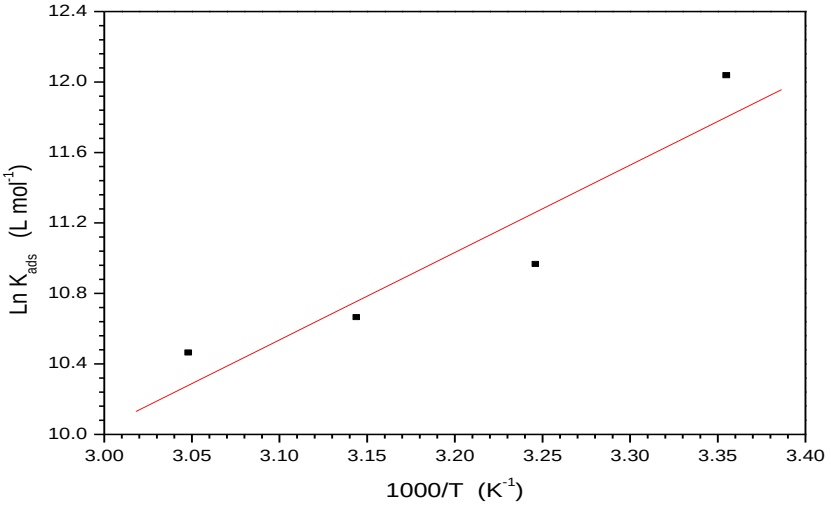

Figure 9: Relationship between Ln (K_{ads}) and 1000/T for Alizarin

ΔH_{ads} is another criterion from which the mode of adsorption based on the absolute value can be probed. Generally, an endothermic process is explicit to chemisorption, while an exothermic adsorption process designates either physisorption or chemisorption [**57**]. In an exothermic adsorption, the adsorption mode is judged based on the absolute value of ΔH_{ads}. The negative sign of ΔH_{ads} indicates that the adsorption of Alizarin inhibitor molecules is an exothermic process (Table 8). It is noted also that the value of the constant K_{ads} decreases with increasing temperature, indicating that the interactions between the adsorbed molecules and the

metal surface are weakened and, consequently, the adsorbed molecules become easily removable. It is obvious that the values of ΔS_{ads} are negative, as inhibitor molecules move freely in the bulk solution before adsorption, while as adsorption progresses, the inhibitor molecules adsorbed onto the mild steel surface become more orderly, resulting in a decrease in entropy [**58-60**] (Table 8).

Table 8: Thermodynamic and kinetic parameters for the adsorption of studied Inhibitors in 1.0 M HCl on the mild steel surface at different temperatures.

T (K)	K_{ads} (L mol^{-1})	ΔG_{ads} (KJ mol^{-1})	ΔH_{ads} (KJ mol^{-1})	ΔS_{ads} (J mol^{-1} K^{-1})
298	1.68×10^{5}	-39.79		-4.96
308	5.756×10^{4}	-38.38	-41.27	-9.38
318	4.257×10^{4}	-38.83		-7.67
328	3.483×10^{4}	-39.50		-5.39

3.5. Quantum chemical calculations

Quantum chemical calculations have been widely used to study relational mechanisms and to interpret the experimental results as well as to resolve chemical ambiguities **[61]**. In this option, the electronic and structural studies of Alizarin were investigated. The quantum chemical parameters have been determined and analyzed in order to explain the interaction between the inhibitor molecules and the metal surface.

3.5.1. Molecular geometry

The molecules structure were built with the Gauss View 3.0 implemented in Gaussian 03 package [**26**], their corresponding geometries were fully optimized at B3LYP/6-31G(d) level of theory. The optimized molecular structure and some geometrical parameters of Alizarin are given in Figure 10 and Table 9 respectively. The HOMO shows that the electronic density is totally localized on the oxygen atoms and the aromatic ring substituted by tow hydroxyl group, the LUMO present a important electronic density distributed over all the molecule (Figure 10).

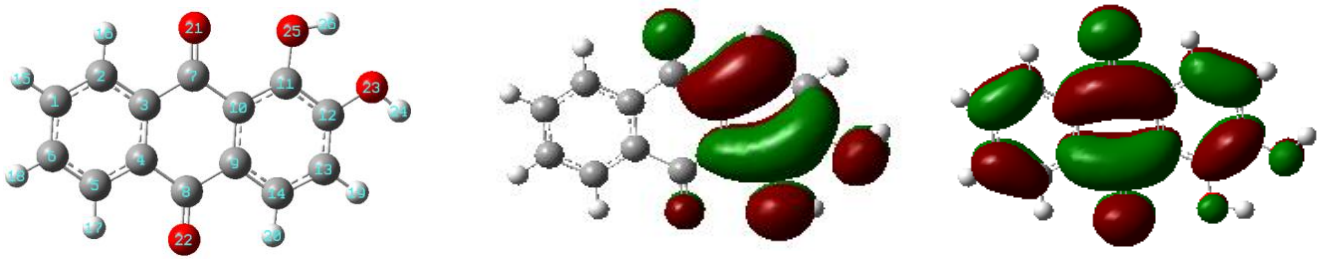

Figure 10: Optimized molecular structure (left), HOMO (center) and LUMO (right) distribution for Alizarin.

From the results given in Table 9 above, it can be notice that the bond length C-C vary between 1.406 Å and 1.499 Å for the bi-substituted ring (by two C=O group). For the aromatic cycle substituted by hydroxyl groups, the bond length values of C-C are lower (1.422-1.387) than the previous ones. The bond length values of C=O and C-OH are 1.225-1.372. For the substituted rings, the bond angle values of C-C-C vary between 117° and 122° which is closely comparable to 120°. The solvent effect can be estimated by the determination of the difference between the geometrical parameters calculated in the gas and aqueous phases. For the inter-atomic distances, the weak effect is observed for the no polarized bond C-C which is about 0.005 Å, whereas this effect is about 0.01Å for C=O polarized bond. The highest effect is observed for C_{12}-O_{23}, its bond length value decreases by about 0.01Å in aqueous phase.

3.5.2. Global molecular reactivity

The calculated electronic parameters from the optimized structure of Alizarin are collected in Table 10. It is found that the value of the ionization potential is 6.214 eV indicating that the molecule has a donor electron power which can be explained by the presence of oxygen atoms and aromatic cycles. While the value of the affinity (2.518 eV) indicated that neutral Alizarin is more stable than its anion and therefore it presents weak acceptor power, this result is in good agreement with the absence of vacant d-orbitals in Alizarin. In addition, it is noted that the value of the dipole moment is μ= 3.186 D indicating that this molecule is strongly polarizable, that polarization increases by 1.265 D in polar solvent (H_2O), as consequence the reactivity of the Alizarin increase in aqueous solution.

Table 9: Some geometrical parameters of Alizarin calculated at B3LYP/6-31G(d) level of theory in gas (G) and in solvent (S).

		Bond lenght (Å)		Bond angle (°)		Bond angle (°)	
Alizarin	G	C3-C7	1.499	C3-C7-C10	117.4	C10-C7=O21	122.7
	S		1.496		117.6		122.7
	G	C7-C10	1.491	C7-C10-C9	120.4	C4-C8=O22	121.1
	S		1.486		120.3		120.8
	G	C9-C10	1.422	C10-C9-C8	121.8	C9-C8=O22	121.2
	S		1.425		121.7		121.3
	G	C8-C9	1.490	C9-C8-C4	117.7	C11-C12-O23	114.1
	S		1.485		117.8		113.9
	G	C4-C8	1.487	C8-C4-C3	120.8	C13-C12-O23	124.4
	S		1.486		120.7		125.0
	G	C4-C3	1.406	C4-C3-C7	122.0	C10-C11-O25	122.3
	S		1.407		121.9		122.5
	G	C10-C11	1.407	C7-C10-C11	121.1	C12-C11-O25	118.3
	S		1.406		121.3		117.8
	G	C11-C12	1.415	C10-C11-C12	119.4		
	S		1.419		119.8		
	G	C12-C13	1.387	C11-C12-C13	121.5		
	S		1.387		121.2		
	G	C13-C14	1.394	C12-C13-C14	119.4		
	S		1.395		119.2		
	G	C14-C9	1.393	C13-C14-C9	120.4		
	S		1.393		120.8		
	G	C7=O21	1.225	C14-C9-C10	121.0		
	S		1.230		120.7		
	G	C8=O22	1.228	C14-C9-C8	117.3		
	S		1.233		117.6		
	G	C11-O25	1.350	C9-C10-C11	118.5		
	S		1.352		118.3		
	G	C12-O23	1.372	C3-C7=O21	120.0		
	S		1.362		119.7		

Moreover, the gap between the LUMO and HOMO energy levels is an important parameter that should be considered. When the energy gap value ΔE decreases the reactivity of molecular system increases [**62**]. The low value of the energy gap indicates that the electron transition from the ground state to the excited ones is favorable. On the other hand, it is a function of reactivity of the inhibitor molecule towards the adsorption on the metallic surface.

The energy gap value (3.696 eV) indicates that the Alizarin is very reactive and can be adsorbed on the metal surface therefore it can be considered as effective corrosion inhibitor. In presence of the solvent the energy gap decreases by 0.185 D, this lets us to conclude that reactivity increases which promotes the electron transition and the charge transfer.

The comparison between the value of hardness (η=1.848) and electronegativity (χ=4.366) shows that the Alizarin molecule interacts easily with the metal surface. In solution, one can notice that the electronegativity increase and the hardness decrease this shows that the Alizarin is more reactive in presence of the solvent, this result can be explained by the strong polarization of the molecule involved by the polar solvent H_2O.

The fraction of electrons transferred (ΔN) from inhibitor to carbon steel surface was also calculated using a theoretical χ_{Fe} and η_{Fe} values for carbon steel of 7 eV mol^{-1} and 0 eV mol^{-1}, respectively [**63**]. The ΔN values are correlated to the inhibition efficiency resulting from electron donation. According to Lukovits et al. study [**64**], if ΔN < 3.6, the inhibition efficiency increases with increasing electron-donating ability at the metal surface. Charge transfer that is of the order of 0.713 shows that Alizarin was a strong electron donor power, this transfer is slightly accentuated by the presence of the solvent.

Table 10: Quantum chemical parameters of Alizarin, calculated at B3LYP/6-31G(d) level of theory in gas and in aqueous (in bold).

	E_{HOMO} (eV)	E_{LUMO} (eV)	ΔE (eV)	μ(D)	I(eV)	A(eV)	χ	η	ΔN
Alizarin	-6.214	-2.518	3.696	3.1863	6.214	2.518	4.366	1.848	0.713
	-6.248	-2.737	3.511	4.4508	6.248	2.737	4.493	1.756	0.726

Conclusion

The inhibition efficiency of mild steel corrosion in 1.0 M HCl by Alizarin has been investigated using weight loss, electrochemical measurements and quantum chemical calculations. The polarization measurements showed that the Alizarin acts as a cathodic type inhibitor and its inhibition efficiency increased with its concentration. EIS measurements also indicate that the inhibitor addition increases the charge transfer resistance and show that the inhibitive performance depends on molecules adsorption on metallic surface. The gravimetric measurement showed that the inhibition efficiency increases with immersion time until 4 h and decreased after this value at 298 K. It is found also that the adsorption of Alizarin obey to the Langmuir isotherm adsorption.

Quantum chemical approach was adequately used to explain the correlation between the mild steel corrosion inhibition and molecular structure of compound. It is found that the corrosion inhibition power of this product is closely related to its quantum chemical parameters. A good correlation is found between the energy of the LUMO and inhibition efficiency. The energy of the lowest unoccupied molecular orbital, E_{LUMO}, is indicative of the ability of the inhibitor molecule to accept electrons. So, the lower the value of E_{LUMO}, the greater the probability the molecule accepts electrons.

References

1. Gupta M., Mishra J., Pitre K.S., *Int. J. Corros.*, 1 (2013) 1–5.
2. Shaban S.M., Saied A., Tawfik S.M., Abd-Elaal A., Aiad I., *J. Ind. Eng. Chem.*, 19 (2013) 2004–2009.
3. Obot I.B, Obi-Egbedi N.O., Umoren S.A., *Corros. Sci.*, 51 (2009) 1868-1875.
4. Lebrini M., Robert F., Vezin H., Roos C., *Corros. Sci.*, 52 (2010) 3367-3376.
5. El Faydy M., Galai M., El Assyry A., Tazouti A., Touir R., Lakhrissi B., Ebn Touhami M., Zarrouk A., *J. Molec. Liq.*, 219 (2016) 396–404.
6. Mihit M., Laarej K., Abou El Makarim H., Bazzi L., Salghi R., Hammouti B., *Arabian. J. Chem.*, 3 (2010) 55-60.
7. El Faydy M., Galai M., Touir R., El Assyry A., Ebn Touhami M., Benali B., Lakhrissi B., Zarrouk A., *J. Mater. Environ. Sci.*, 7 (4) (2016) 1406-1416.
8. Ghailane T., Balkhmima R.A., Ghailane R., Souizi A., Touir R., Ebn Touhami M., Marakchi K., Komiha N., *Corros. Sci.*, 76 (2013) 317–324.
9. Abboud Y., Abourriche A., Saffaj T., Berrada M., Charrouf M., Bennamara A., Cherqaoui A., Takky D., *Appl. Surf. Sci.*, 252 (2006) 8178–8184.
10. Benhiba F., Zarrok H., Elmidaoui A., El Hezzat M., Touir R., Guenbour A., Zarrouk A., Boukhris S., Oudda H., *J. Mater. Environ. Sci.*, 6 (8) (2015) 2301-2314.
11. Oguzie E., Akalezi C., Enenebeaku C., *Pigm. Res. Technol*., 38 (2009) 359–365.
12. Ebenso E.E., Oguzie E.E., *Mater. Lett.*, 59 (2005) 2163–2165.
13. Ebsenso E.E., Alemu H., Umoren S.A., Obot I.B., *Int. J. Electrochem. Sci*., 3 (2008) 1325–1339.
14. Deng S., Li X., Fu H., *Corros. Sci*., 53 (2011) 3596–3602.
15. Ben Hmamou D., Salghi R., Zarrouk A., Zarrok H., Hammouti B., Al-Deyab S.S., Bouachrine M., Chakir A., Zougagh M., *Int. J. Electrochem. Sci*., 7 (2012) 5716 – 5733.
16. Oguzie E., Unaegbu C., Ogukwea C.N., Okolue B.N., Onuchuku A.I., *Mater. Chem. Phys*., 84 (2004) 363–368.
17. Mohan P., Paruthimal Kalaignan G., *J. Mater. Sci. Technol*., 29 (2013) 1096–1100.
18. El Hezzat M., Assouag M., Zarrok H., Benzekri Z., El Assyry A., Boukhris S., Souizi A., Galai M., Touir R., Ebn Touhami M., Oudda H., Zarrouk A.Der Pharma Chemica, 7 (2015) 77-88.
19. El Assyry A., Benali B., Lakhrissi B., El Faydy M., Ebn Touhami M., Touir R., Touil M., Res. Chem. Inter., 41 (2015) 3419-3431.
20. ASTM G-81, Annual Book of ASTM Standards, (1995).
21. Stern M., GearyA.L., *J. Electrochem. Soc*., 104 (1957) 56.
22. Lee C., Yang W., Parr R.G., *Phys. Rev. B*, 37 (1988) 785–789.
23. Becke A.D., *J. Chem. Phys*., 98 (1993) 1372–1377.

24. Frisch M.J., Trucks G.W., Schlegel H.B., Scuseria G.E., Robb M.A., Cheeseman J.R., Montgomery J.A., Vreven T., Kudin K.N., Burant J.C., et al., Gaussian 03, Revision B.01, Gaussian, Inc., Pittsburgh, PA, 2003.
25. Obi-Egbedi N.O., Obot I.B., El-Khaiary M.I., *J. Mol. Struct*., 1002 (2011) 86-96.
26. Cances E., Mennucci B., Tomasi J., *J. Chem. Phys*., 107 (1997) 3032–3042.
27. Pearson R.G., *Inorg. Chem.*, 27 (1988) 734–740.
28. AbdelAal M.S., Radwan S., El Saied A., *Br. Corros. J.*, 18, 2 (1983).
29. Chaudhary R.S., Sharma S., *Indian J. Chem. Technol*., 6, 202 (1999).
30. Bentiss F., Traisnel M., Lagrenée M., *Appl. Surf. Sci*., 161, 196 (2000).
31. Abdallah M., *Corros. Sci*. ,44 (2002) 717.
32. El Faydy M., Galai M., El Assyry A., Tazouti A., Touir R., Lakhrissi B., Ebn Touhami M., Zarrouk A., *J Molec. Liq.*, 219 (2016) 396–404.
33. Touir R., Ebn Touhami M., Larhzil H., protection of galvanized steel in 3.0 % NaCl solution by SG/CTAB, LAP LAMBRT Acadimic Publishing, Saarbrucken 2016, Deutschland/Germany.ISBN: 978-3-659-9392-6.
34. Rochdi A., Touir R., El Bakri M., Ebn Touhami M., Bakkali S., Mernari B., *J Envir. Chem. Engin*., 3 (2015) 233–242.
35. Rochdi A., Kassou O., Dkhireche N., Touir, R., El Bakri M., Ebn Touhami M., Sfaira M., Mernari B., Hammouti B, *Corros. Sci.*, 80 (2014) 442-452.
36. Umoren S.A., Ebenso E.E., Okafor P.C., Ekpe U.J., Ogbobe O., *J. Appl. Polym. Sci*., 103 (2007) 2810-2816.
37. Popova A., Sokolova E., Raicheva S., Christov M., *Corros. Sci*., 45 (2003) 33-58.
38. Elayyachy M., Elkodadi M., Aouniti A., Ramdani A., Hammouti B., Malek F., Elidrissi A., *Mat. Chem. Phys*., 93 (2005) 281-285.
39. Szauer T., Brand A., *Electrochim. Acta* , 26 (1981) 1253-1256.
40. Gerengi H., Darowicki K., Bereket G., Slepski P., Corros. Sci. 51 (2009) 2573-2579.
41. Noor E.A., *Int. J. Electrochem. Sci*., 2 (2007) 996-1017.
42. Singh A.K., Quraishi M.A., *Corros. Sci*., 53 (2011) 1288-1297.
43. Singh A.K., Shukla S.K., Singh M., Quraishi M.A., *Mater. Chem. Phys*., 129 (2011) 68-76.
44. Li X.H., Mu G.N., *Appl. Surf. Sci*., 252 (2005) 1254–1265.
45. Benabdellah M., Aouniti A., Dafali A., Hammouti B., Benkaddour M., Yahyi A., Ettouhami A., *Appl. Surf. Sci*., 252 (2006) 8341–8347.
46. Noor E.A., Al-Moubaraki A.H., *Mater. Chem. Phys*., 110 (2008) 145–154.
47. Subramanyam N.C., Mayanna S.M., Corros. Sci., 25 (1985) 163-169.
48. Eldakar N., Nobe K., Corrosion 36 (1981) 271-278.
49. Kurosawa K., Fukushima T., *Corros. Sci*., 29 (1989) 1103-1114.
50. Kuznetsov Yu.I., *Prot. Met.*, 37 (2001) 101–107.
51. Deng S.D., Li X.H., Fu H., *Corros. Sci*., 53 (2011) 760–768.
52. Cano E., Polo J.L., La Iglesia A., Bastidas J.M., *Adsorption*, 10 (2004) 219–225.
53. Badiea A.M., Mohana K.N., *Corros. Sci*., 51 (2009) 2231-2241.
54. Szklarska-Smialowska Z., Mankowski J., *Corros. Sci*., 18 (1978) 953-960.
55. Yurt A., Ulutas S., Dal H., *Appl. Surf. Sci*., 253 (2006) 919-925.
56. Hongbo F., *Chemical Industry Press, Beijing*, (2002) p. 166.
57. Durnie W., Marco R.D., Jefferson A., Kinsella B., *J. Electrochem. Soc*., 146 (1999) 1751-1756.
58. Mu G., Li X., Liu G., *Corros. Sci*., 47 (2005) 1932.
59. Zarrouk A., Zarrok H., Salghi R., Hammouti B., Bentiss F., Touir R., M. Bouachrine, *J. Mater. Environ. Sci.*, 4 (2) (2013) 177-192.
60. Aouine Y., Sfaira M., Ebn Touhami M., Alami A., Hammouti B., Elbakri M., El Hallaoui A., Touir R., Inter. J. Electrochem. Sci. , 7 (2012) 5400-5419.
61. Wang D., Li S., Ying Y., Wang M., Xiao H., Chen Z., *Corros. Sci*., 41 (1999) 1911–1919.
62. Kraka E., Cremer D., *A New Enediyne Warhead, J. Am. Chem. Soc*., 122 (2000) 8245 -8264.
63. Obot I.B., Obi-Egbedi N.O., *Corros. Sci*., 52 (2010) 657–660.
64. Lukovits I., Kalman E., Zucchi F., *Corrosion*, 57 (2001) 3–9.